Dosimetric Pitfalls for Relative Dosimetry in Electron Disequilibrium Region

Timothy C Zhu

Department of Radiation Oncology, University of Pennsylvania, Philadelphia, PA

I Introduction

Various types of radiation detectors are used to measure relative dose distributions for therapeutic electron and photon beams. Most detectable signals from a radiation detector are correlated to the energy imparted $\delta\varepsilon$ to the detector [1]. This, in turn, is related to the absorbed dose in the detector, D_{det}. Table I lists types of radiation detectors, their signals, and their relationship to the dose in the sensitive volume of the detectors. The meaning of the dosimetric quantities can be found in Refs. 2 – 4. In this review we will only consider the first three types of detectors, especially ionization chambers and diodes, since they are the most commonly used in acquiring beam data.

Table 1. Example of radiation detectors

Type	Measured Quantities	Relation to D_{det}
Ionization chambers	Charges (Q)	$D_{det} = (W/e)_{air} \cdot Q/m \cdot \beta$
Si Diode detectors	Charges (Q)	$D_{det} = (W/e)_{Si} \cdot Q/m \cdot \beta$
TLD	Light intensity (I)	$D_{\det} \propto \int I dt$
Fricke dosimeter	Fe^{3+} content (ΔA)	$D_{det} = \Delta A/\rho l (e_m)_t G_t$
Film	Optical density (OD)	$D_{det} \propto OD$
Calorimetry	Temperature (ΔT)	$D_{det} = c_p \cdot \Delta T$

When such a measuring device is introduced into a radiation field, it tends to disturb the field. For relative dosimetry, one major concern is the spatial resolution of the detector since the signal correlates to the integral (or mean) dose in the detector and we are interested in the dose in the medium at one point. This correction can be done using the concept of detector convolution kernel. This is somewhat different from conditions for absolute dosimetry where the electron fluence distribution over the detector tends to be uniform (although not always possible)! Nevertheless, we will discuss the correlation between the two situations from the fundamental level. One of the most relevant perturbation factors is the displacement factor caused by replacing the medium by the detector (e.g. an air volume for ionization chamber).

Due to the lack of a general methodology to correct for the complicated perturbation under electron disequilibrium, specific recommendation of the types of detectors and correction methods differ for different situations. We will focus on the following three areas of relative dosimetry: 1. Profile measurement, where the intention is to measure the lateral fluence distribution including the penumbra region of a radiation beam. 2. Depth dose measurement for electrons or in the buildup region for photons, where the dose gradient is steep. 3. Small field dosimetry, where the output on the central axis may be affected by the penumbra of the small field.

For dynamically modulated photon beams, the profile is usually measured by a detector array. Here, the important correction is the relative sensitivity between different detectors. We will discuss the relative sensitivity calibration of the detector array.

II. Perturbation factors and detector convolution kernel

Let us briefly review the treatment of perturbation factors for absolute dosimetry and then expand it to electron disequilibrium regions using the concept of detector convolution kernel. Excellent reviews for absolute dosimetry can be found in that of Nahum [5], Alm Carlsson [1], and Svensson and Brahme [6]. However, there are few papers on the perturbation factors under electron disequilibrium conditions.

If the detector is small compared to the range of the charged particles (i.e. it behaves as a Bragg cavity), one can write [5]

$$D_{med}(P) = \overline{D}_{\det} \cdot s_{med,\det} \cdot p\,, \qquad (1)$$

where p is the perturbation of the electron fluence, $s_{med,det}$ is the mass collision stopping power ratio between medium and the detector material. Note that the dose to the medium has been written as $D_{med}(P)$ to indicate that the value required is at a specific position P, which can be shifted from the center of the detector. $\overline{D}_{\det}$ is the mean dose in the detector. This expression is valid under electron disequilibrium, where $\overline{D}_{\det} \neq \overline{K}_{\det}$. Nahum [5] pointed out that the cause of p is the perturbation of the secondary electron fluence in the medium:

$$p = \frac{\int_{\Delta}^{\Delta} (\Phi_E)^P_{med} (L_\Delta / \rho)_{\det} dE + [(\Phi(\Delta)^P_{med} (S(\Delta)/\rho)_{\det} \cdot \Delta]}{\int_{\Delta}^{\Delta} (\Phi_E)_{\det} (L_\Delta / \rho)_{\det} dE + [(\Phi(\Delta)_{\det} (S(\Delta)/\rho)_{\det} \cdot \Delta]},$$

where Φ_E is the electron fluence and L_Δ/ρ is the restricted stopping power ratio, all other quantities have their usual meaning [4]. For absolute dosimetry (under electron equilibrium) this perturbation factor is usually very small (a few percent) so that one can separate it into multiplication of several independent perturbation factors. This separation is not usually possible in electron disequilibrium regions where the perturbation can be much larger. One of the most common separations is the wall correction factor and displacement factor [7]. The displacement (or replacement) factor is further separated into electron fluence correction and gradient correction according to TG21 [7]. Bjärngard and Kase [8] argues that this latter separation is non-physical because it violates Fano's theorem [9].

The displacement factor describes the perturbation caused by replacing the medium by the detector active medium (for ionization chamber, an air cavity without the wall). There are two alternative approaches to deal with this effect: either as a multiplicative correction factor or by referring the position of measurement to some other depth than that of the center of the cavity. Cunningham and Sontag (1980) used the first approach and carried out an experimental and theoretical study of the displacement factor for Farmer-type ionization chamber with different radius [10]. They concluded that this is caused by missing scatter and attenuation in the cavity. Figure 1 showed that as they insert Lucite sleeves of different radial increments into the chamber until the cavity is completely filled, the displacement factor reduces accordingly. The crosses are from measurement in a lucite phantom using the lucite sleeves for cobalt-60 radiation and a beam from a 25 MV linear accelerator. The solid lines are from the "least square" fit to the crosses in each case and the dashed lines represent calculations considering primary and once-scattered radiation only. The curve shape of the displacement factor agrees with the first-scatter and attenuation calculations. AAPM TG21 uses their values as a function of inner diameter of the chamber and x-ray energy. Other experimental values have been given by Johansson *et al* for ^{60}Co up to 42 MV x-rays. They found the displacement factor, $P_{dis} = 1 - k \cdot r$, depends significantly on photon energy and cavity radius but not on depth ($d > d_{max}$) or field size [11]. For the radius expressed in millimeters, Johansson *et al*'s *k*-values were 0.40, 0.40, 0.31, 0.24, and 0.25 for ^{60}Co, 5 MV, 8 MV, 16MV and 40 MV photon radiation, respectively [11].

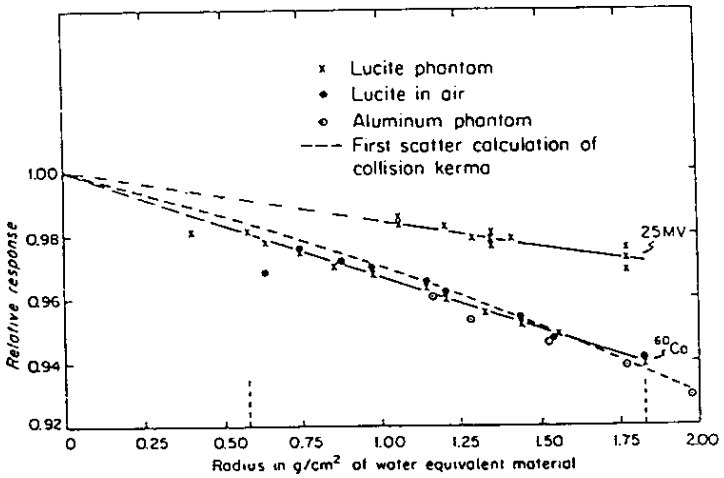

Fig. 1 Relative response of a Farmer-type ion chamber (from Cunningham and Sontag, 1980). Smaller air volume to the left.

A different approch uses effective point of measurement to correct the displacement perturbation. This was first suggested by Skaggs for electron beam [12]. Hettinger *et al* extended the idea to megavoltage photon beams [13]. Figure 2, taken from IAEA code (1987) [14], illustrates clearly all the concepts involved. If the secondary electrons are predominantly forward-directed, then a cylindrical cavity will effectively measure at some point upstream of its center. An implicit assumption behind the use of P_{eff} is that the displacement is the same for all electron energies in the fluence spectrum. P_{eff} is assumed to be the back of the front window for a parallel-plate chamber.

Dutreix and Bridier showed that the shift is $8r/3\pi$ (= $0.85r$) for a cylindrical cavity, assuming the secondary electrons are generated in the forward direction and the number of ions is proportional to the chord length of the electrons in the cavity [3]. Svensson and Brahme proposed a further modification to take into account of the angular spread of the electrons [6]. Various researchers have measured the size of the upstream shift of P_{eff} from the cavity center by comparing the readings of cylindrical chambers with various radii with that of a parallel-plate chamber. Andreo has summarized the various experimental result in Table 2 [15]. IAEA code

recommends values of $Z_{P_{eff}} - Z_P$ as *0.5r* for electron beams and ^{60}Co, *0.75r* for high-energy photon beams, *0.35r* for ^{137}Cs, and 0 for orthovoltage x-rays [14].

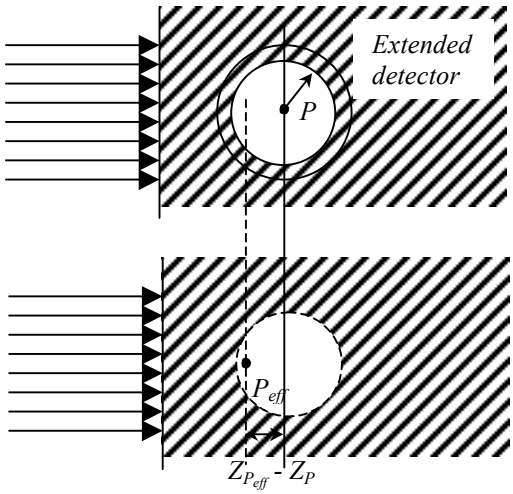

Fig. 2. Displacement of the effective point of measurement P_{eff} from the center P of an ionization chamber.

Table 2. The shift of the effective point of measurement (from Ref. 15)

References	Depths < d_{max}	Depths ≥ d_{max}	Photon beam
Hettinger *et al* [13]	*0.75r*		34 "MV"
Dutreix [16]	*0.85r*		5.5 & 24 "MV"
Johansson *et al* [11]	*0.75r – 0.95r*	*0.5r – 0.8r*	^{60}Co – 42 "MV"
McEwan [17]		*0.6r – 0.8r*	^{60}Co & 30 "MV"
Zoetelief *et al* [18,19]		*0.75r*	^{60}Co
Svensson and Brahme [6]		*0.55r*	^{60}Co & 5 "MV"

The advantage of the concept of effective point of measurement is that one can use it in the buildup region. This is useful for depth dose measurement for electron beams. However, unlike displacement correction factor, this concept is only valid for a monodiretional beam, e.g. not for two opposed parallel beams [3]. It is also impossible to extrapolate surface dose for x-rays using either methods. A further extension of the concept, which avoids the above-mentioned drawbacks, is the detector convolution kernel.

Supposing that a detector is introduced into a medium under a radiation field, the dose disturbance of the detector can be generally expressed as

$$\overline{D}_{\text{det}} = \iiint g(\mathbf{r}-\mathbf{r}') \cdot D_{med}(\mathbf{r}')d\mathbf{r}' \qquad (2)$$

where $g(\mathbf{r})$ is the detector convolution kernel, $\overline{D}_{\text{det}}$ is the mean dose determined by the detector, and D_{med} is the dose in the medium. Compared to Eq. (1), $g(\mathbf{r})$ describes the additional dose average effect of an extended detector volume. g must have an finite range reflecting the size of the detector and the range of secondary electrons. In principle, g can include all the detector disturbance, which cannot be separated into independent effects like wall correction and displacement correction. We will not explore here how to determine g theoretically since it relates doses (or secondary electron fluences) with and without the detector and is thus extremely complicated. One could, however, try to determine g experimentally for a specific radiation quality. As a first order of approximation, Eq. (2) can be simply considered as an average of the dose distribution in the medium with a weighting function, g, that depends on the detector perturbation. This corresponds to the gradient correction used in TG21. The convolution formalism assumes that g has the same shape everywhere within a given radiation quality.

If one only considers dose measurement in the buildup region and the lateral fluence distribution is uniform, the detector convolution kernel will become a one-dimensional function (also called line spread function) $g(z)$, i.e.

$$\overline{D}_{\text{det}} = \int g(z-z') \cdot D_{med}(z')dz' \qquad (3)$$

This equation can be solved by deconvolution of two measured depth dose curves, one using the detector with extended volume, the other with a parallel-plate ionization chamber or diode without extended volume in z direction. As indicated above with the concept

of effective point of measurement, the peak of *g* must be shifted towards the radiation source, i.e. it depends on the direction of the primary radiation. If multiple beams are used, then *g* must be different for each beam and the final result of convolution can be summed together. We will discuss its application further in section III.

The concept of detector convolution kernel is more useful for correcting profile measurement in regions with steep gradients because *g* can be independently measured. Extensive literature exists on the experimental determination of *g* [20-24]. All measurement techniques take advantage of the ability to modify the lateral fluence distribution of the radiation, thus D_{med}. Figure 3 shows the shape of the detector convolution kernel for two thimble ionization chambers (*Wellhöfer* IC-10 and IC-3) and a p-type Scanditronix diode (2.5-mm diameter). These measurements were made using a 6-MV step x-ray field and the two-dimensional detector response kernels are assumed to be cylindrically symmetric. We find that the following function fits the data best:

$$g(r) = \frac{3}{2\pi R^2}\sqrt{1 - r^2/R^2} \qquad \text{for ionization chambers} \qquad (4)$$

$$g(r) = \frac{1}{\pi w^2} e^{-r^2/w^2} \qquad \text{for diode}$$

The kernels are normalized using $2\pi \int g(r) r dr = 1$. Dawson *et al* found a substantial correlation between the effective radius, *R*, and beam energy, which tends to increase with increasing photon energy [25]. We will discuss this application further in sections IV and V.

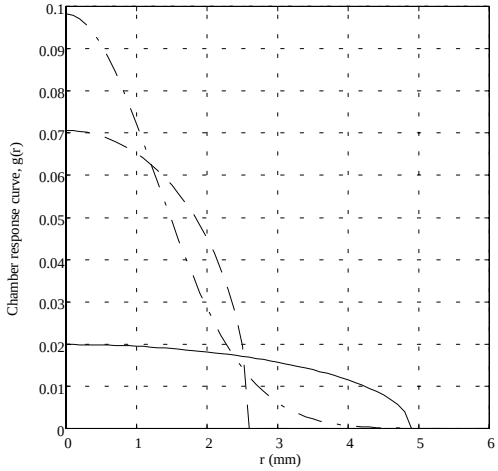

Fig. 3. Detector convolution kernel *g(r)* measured for *Wellhöfer* 0.1 cc IC-10 (solid) and 0.03 cc IC-3 (dashed) ion chambers, and a Scanditronix p-type diode (dash-dotted).

III Depth dose measurement

Photons

The golden standard for dose measurements in the buildup region is the extrapolation parallel-plate chamber. However, these measurements are time consuming. Silicon diodes with small active volume in the radiation direction has been found to have little perturbation effect [26]. Without special correction, a thimble-type ionization chamber overestimates the dose in the buildup region because of its relatively large volume. Figure 4 compares the depth dose measured for an 18-MV x-ray from a Varian 2100CD accelerator by a *Wellhöfer* IC-10 ionization chamber (solid line) and a Scanditronix p-type photon diode (dashed line). The difference is clearly illustrated. However, if one convolves the diode result with the detector convolution kernel of the IC-10 chamber obtained in Fig. 3 (solid line) the resulting curve coincides with the ionization chamber result (Fig. 4, dotted line). Here, the peak of *g* is shifted away from surface by *0.1r*. This means that the distortion by ionization chamber can be explained by the detector convolution kernel.

A parallel-plate chamber with fixed plate separation can also be used to measure the depth dose in the buildup region. However, correction is needed for the fixed plate separation. Velkley *et al* studied the relationship between the correction factor and plate separation for an extrapolation parallel-plate chamber at different depths and photon energies. They found that the parallel-plate chamber with fixed plate separation tends to overestimate dose in the buildup region [27]. They were the first to introduce a correction factor ξ in the form of [27]

$$P'(d) = P(d) - \xi(E, d/d_{\max}) \times l, \qquad (5)$$

where *l* is plate separation, *d* is depth to front surface of chamber, *P'* is corrected percentage buildup, and *P* is the percentage buildup obtained with chamber with plate separation *l*. ξ decreases with increasing photon energy and increasing depth for a fixed photon energy. For their particular extrapolation chamber design, Velkley *et al* found ξ to be 4.5%/mm, 3%/mm, 1.6%/mm, and 1%/mm for ^{60}Co, 4MV, 8MV, and 25MV, respectively, on the surface.

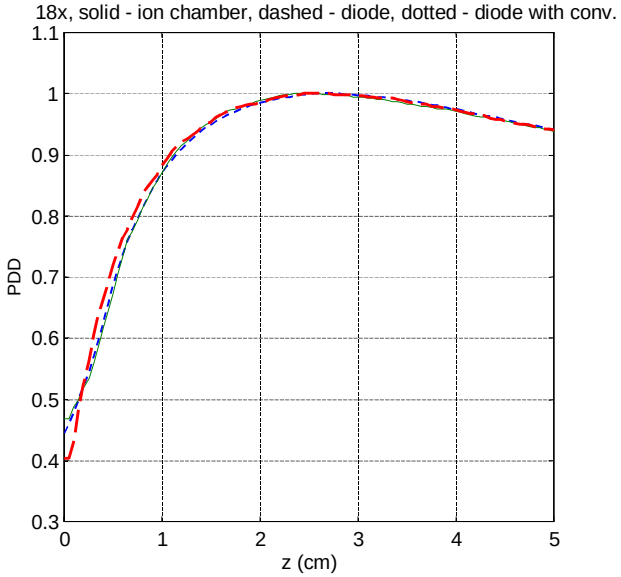

Fig. 4 PDD measured for 18 MV x-rays using *Wellhöfer* IC-10 ionization chamber (solid), Scaditronix diode (dashed) and the diode result convolved with the detector convolution kernel for the ionization chamber. Collimator setting is 20 × 20 cm^2, SSD = 100 cm.

Nilsson and Montelius [28] performed one of the most extensive studies of the fluence perturbation of parallel-plate ionization chamber under electron disequilibrium conditions and concluded that it is not possible to correct the perturbation effect in one parallel-plate chamber with fixed plate separation with correction factors obtained with extrapolation chambers of other dimensions. They showed that even after applying the correction method suggested by Velkley *et al*, the surface dose measured by a parallel-plate chamber of 5-mm diameter was still overestimated by a factor of 2. The electron fluence perturbation varies both with side wall material and chamber geometry (e.g. chamber diameter, guard width, and plate separation). They concluded that the major source of perturbation in a parallel-plate chamber is the in-scattering of electrons through the side walls and to some extent backscattering from the back of the chamber. They also found that the extrapolation of ionization to zero separation is not linear for small plate separations [28]. Monte Carlo simulation for parallel-plate chamber perturbation effect has been performed but only for depths beyond d_{max} [29].

Correction factors ξ for specific chambers have been experimentally determined by Mellenberg [30] for the Markus chamber (PTW 30-329), Gerbi [31] for the Attix chamber, and Gerbi and Khan [32] for a range of commercially available fixed-separation parallel-plate chambers (Capintec PS-033, the PTW 30-329 Markus chamber, and Memorial chambers with circular or rectangular electrodes). Gerbi and Khan [32] concluded that the Velkley correction (Eq. (5)) produces acceptable results (within 2%) for all chambers but the Marcus chamber, because of its small guard, is still on average 11%, 6%, and 3.7% too high after correction for ^{60}Co, 6MV, and 10MV photon energies, respectively. For higher photon energies, the Velkley correction works well (within 2%). Mellenberg [30] produced an extensive table of correction factors for the Markus chamber, which is expressed as a constant term (second term of Eq. (5)). Rawlison *et al* reviewed Velkley correction factors for commercially available parallel-plate chambers and pointed out that Velkley's formula needs to be modified to include influence of the chamber geometry and density of wall material.[33] They provided an improved formula:

$$P'(d) = P(d) - c(E)\cdot(l/w)\cdot\rho^{0.8}e^{-4.0d/d_{\max}} \qquad (6)$$

where *w* is the inner diameter of wall, ρ is density of wall material (g/cm^3), *c(E)* = 43%, 27%, 15% for Co-60, 6MV, 18MV, respectively. All other parameters are the same as Eq. (5). This modified equation works well even with the Markus chamber. Gerbi and Kahn [34] recently also examined chamber response in the buildup region for obliquely incident photon beams and found that the overresponse also changes with incident angle. They recommend to use an extrapolation chamber or a well-guarded fixed-separation plane-parallel ionization chamber with a plate separation of 1 mm or less. The overresponse for the Attix chamber (plate separation 2.5 mm) at surface is the smallest among all the commercially available chambers and is 1.12 with little angular dependence for 6 MV x-ray. Here, the overresponse is defined as a ratio of measured *PDD(d)* between fixed separation and extrapolation chambers. Gerbi and Kahn found that TLD is a good dosimeter for buildup measurement even with oblique incident angle [34].

Another important correction factor for parallel-plate ionization chamber is the polarity effect, which can be easily corrected by averaging the charges for both polarities. Several references discuss its origin [35-38] Gerbi and Kahn [39] and Aget and Rosenwald [36] give the polarity effect for several commercially available chambers for photon and electron beams.

Electrons

Extensive works on the perturbation effect of parallel-plate chamber for electrons exist primarily because it is the preferred detector for low energy electron beam absolute dosimetry [5]. The perturbation produced by in-scatter from side wall was found to exist even at d_{max}. The total perturbation according to Eq. (1) (including wall and electron fluence correction), has been experimentally determined to be a function of mean electron energy at depth, E_z. For well-guarded parallel-plate chambers, e.g. NACP chamber, $p \approx 1$. For Marcus chamber, Nahum [5] found that the compiled data agrees well with that from AAPM TG39 [40], i.e.

$$p = 1 - 0.041 \cdot e^{-0.4E_z}. \qquad (7)$$

Here E_z is in MeV.

Figure 5, taken from Ref. [41], shows electron fluence perturbation on the front surface of an air cavity in a PMMA phantom at depth of maximum dose for 6 MeV electron beam. This perturbation is much more serious than that for a photon beam (see for example Ref.[28]). A well designed guard ring can eliminate the effect of excess scattering near the side wall, thus producing a perturbation-free chamber.

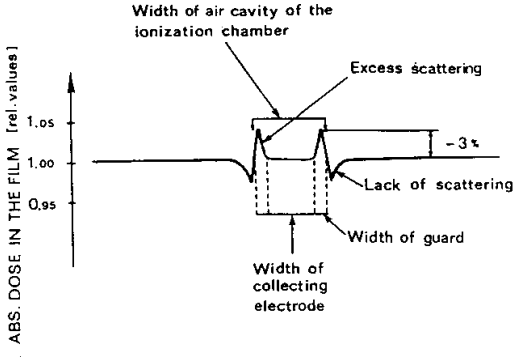

Fig. 5 Film measurement across the front surface of an air cavity in a PMMA phantom at d_{max} for 6 MeV electrons.

For a thimble-type ionization chamber, the best correction method for electron depth dose measurement is shifting the effective depth of measurement by *0.5r* for all energies [14]. Detailed study using the detector convolution kernel remains to be done. One other necessary correction for gas-filled ion chambers is the energy dependence of the water-to-air stopping power ratio.[2] This dependence is almost entirely due to the effect of the density or polarization effect [42], reducing the collision stopping power in water but not in air [5]. This problem disappears for non-gaseous detector materials such as TLD and Si diode.

IV Penumbra measurement

Artificial broadening caused by the detector size is illustrated in Fig. 6, taken from Ref. [20]. Dawson *et al* studied the relation between penumbra width and ionization chamber inner diameter for a series of specially designed chambers with inside diameter varying between 0.3 to 1.4 cm [25]. They concluded that the P20-80 or P10-90 penumbral degradation associated with the inside diameter of the chamber can be corrected using a standard slope of 0.5 cm/cm inside diameter, regardless of the chamber type and radiation quality. Metcalfe *et al* [43] compared penumbra measured with ionization chambers, TLD, Scanditronix diode, and film and concluded that the diode (2.5 mm diameter) gives result consistent with film and very closely (within 0.2 mm) models the response of a point detector. TLD (1×1×6 mm) gives better result. We have tested a new 0.03 cm^3 ionization chamber (Wellhöfer IC-3 with 4-mm inner diameter) for penumbra measurement and found the result agrees with diode to within 0.5 mm.

Existing studies have proven definitively that the detector convolution kernel can explain the broadening of the measured penumbra due to the detector size [20-25]. It is possible to extrapolate the true penumbra using the detector convolution kernel. However, the current deconvolution algorithm is very susceptible to noise and requires manual tuning to eliminate the noise effect [23]. This problem should be solvable if both the penumbra and detector convolution kernel are expressed as analytical functions. Several studies give various analytical expressions for the penumbra [43,44] and the detector convolution kernel (Eq. (4)).

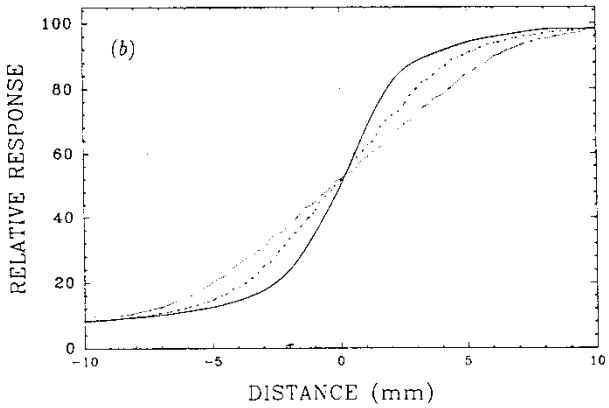

Fig. 6. Penumbra for a 6 MV x-ray beam obtained with 9.5 mm (dotted) and 5.8 mm (dashed) inner diameter ionization chamber. Full curve is measured with film.

V Small field dosimetry

For beam data characterization of stereotactic cones (e.g. *TMR*, *OF*, and Profiles), the detector size effect is critical. Detector convolution kernel can still be used, but unlike one-dimensional penumbra measurement, one has to consider the effect in two-dimensions. Because the penumbra for small field may cut into the central-axis, the output can also decrease as a result. These effects can be expressed using detector convolution kernel as [45]

$$F(x,y) = \iint g(x-x', y-y') \cdot f(x',y')dx'dy' \quad (8)$$

where *F(x,y)* is the measured profile, *f(x,y)* is the true profile, and *g* is the detector convolution kernel. On the central-axis, the reduction of output factor, *CF*, can be expressed as [45]

$$CF = F(0,0) = \iint g(x',y') \cdot f(x',y')dx'dy' \quad (9)$$

Figure 7 compares calculated and measured correction factors for ionization chambers with detector convolution kernel described in Fig. 3. Here we have assumed that both *g* and *f* are cylindrically symmetric, i.e., they are a function of $\sqrt{x^2+y^2}$. Deconvolution for Eq. (8) with cylindrical symmetry can be performed using inverse Abel transform. [46]

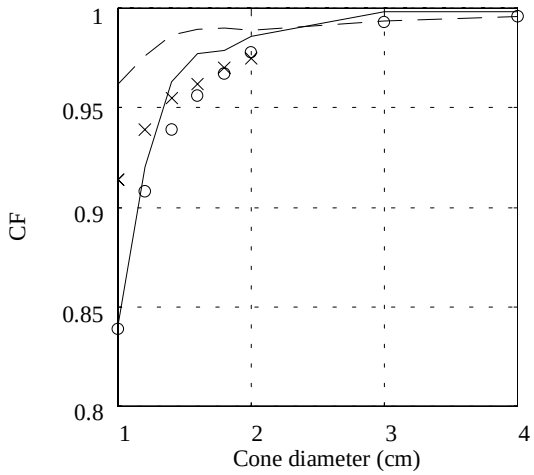

Fig. 7 Comparison between theoretical and measured *CF* for chambers. Lines (solid for 0.1 cc chamber, dashed for 0.03 cc chamber) are calculation using Eq. (9). Symbols (circle for 0.1 cc chamber and cross for 0.03 cc chamber) are measured *CF*, determined by the ratio of output measured by ionization chamber to that measured by diode.

Several studies have been performed to compare the output factors measured for the stereotactic cones by various detectors [47-49]. Table 3 lists the results for relative output factors for a 6MV x-rays from a Clinac 2500 accelerator [49]. Serago *et al* [49] concluded that small diode and TLD seem to be the appropriate choices of radiation detectors to determine relative dose for small field sizes. Bjärngard *et al* performed Monte-Carlo simulation and found the diode detector breakdown for cone diameter less than 0.5-cm [47].

Table 3. Relative output factors for 6 MV x-rays measured with ionization chamber (IC), diode, TLD, and film

	Chamber /detector						
	IC	IC	IC	IC	Diode	TLD	Film
Field size	0.6 cm^3	0.125 cm^3	Markus	Soft x-ray	2 mm	3 × 3 mm	XV-2
10×10 cm	1.00	1.00	1.00	1.00	1.00	1.00	1.00
Diameter							
8.0 mm					0.76	0.73	0.74
11.0 mm			0.74	0.72	0.82	0.80	0.80
14.0 mm		0.75	0.83	0.80	0.85	0.85	0.85
17.5 mm		0.82	0.87	0.85	0.88	0.87	0.88
21.0 mm	0.76	0.87	0.90	0.89	0.89	0.88	0.90
24.0 mm	0.84	0.90	0.91	0.91	0.90	0.90	0.91
26.5 mm	0.89	0.92	0.92	0.92	0.91	0.90	0.92
31.5 mm	0.92	0.92	0.93	0.93	0.91	0.91	0.92
36.5 mm	0.93	0.93	0.93	0.93	0.92	0.92	0.92

VI Detector array

With increasing popularity of dynamic radiotherapy, it becomes necessary to develop linear detector arrays to measure the dose profile. Point measurement gives the most accurate dose distribution but it is very time-consuming because the dose at each measurement point must be obtained by integrating during the entire exposure. A few commercially available detector arrays exist in the market; they are the Scanditronix diode array [50], Wellhöfer multichamber array [51], and Sun Nuclear Profiler [52]. All commercially available detector arrays are adequate for dynamic wedge dosimetry and should work for dynamic modulated photon beams. One side advantage of the detector array is the speedup for static beam dosimetry, which makes them suitable for quick routine QC [53]. There is no published evaluation of the accuracy of the detector array for electron beam dosimetry but one would favor diode array because of its good spatial resolution and nearly constant stopping power ratio relative to water.

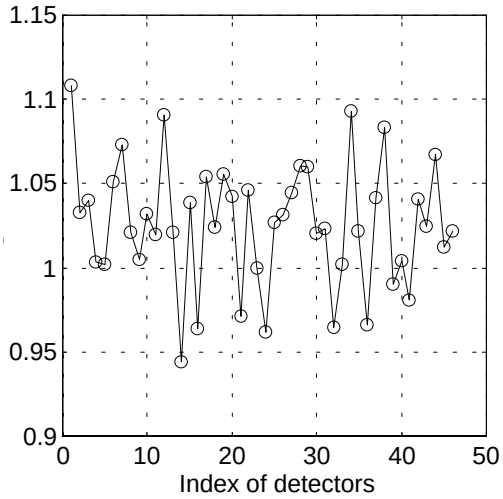

Fig. 8 Relative sensitivity for the individual diodes used in the Profiles. Taken from Ref. [52]

One crucial step for the use of detector array is the calibration of the relative sensitivity of detectors. Figure 8 shows the sensitivity difference between individual diode is as much as ±10%. In general the dose determined by the detector array can be expressed as:

$$D_i = a \cdot CF_i \cdot Q_i, \qquad (10)$$

where a is an arbitrary constant, CF_i is relative calibration factor of each detector, Q_i is the charge reading of each detector. Two methods are used to measure CF_i. One can use a narrow beam and move each detector to the center of the beam. CF_i can be determined by ratio of the charge Q_i assuming that the dose delivered is the same. The recently introduced broad-beam calibration procedure [54] uses a large open field that covers all detectors. Radiation is delivered to the array and the readings of the detectors are saved in a data array labeled as [C]. The array is then moved laterally along the array axis such that the detectors now occupy positions in the fields formerly occupied by the adjacent detectors. Another dose is delivered and the readings are saved in a data array [D]. If the dose delivered is precisely the same for both [C] and [D], then the relative sensitivity of neighboring detectors can be calculated as a ratio of their charges. For example, the array was shifted for [D] and #2 (detector number 2 in the array) occupies #1's former position during [C]. Then the sensitivity ratio of #2 to #1 is D2/C1. Likewise the sensitivity ratio of #3 to #2 is D3/C2,

and the sensitivity ratio of #3 to #1 is (D3/C2)(D2/C1). Therefore one can obtain the ratio of sensitivity relative to #1 for all detectors.

VII Concluding Remarks

The perturbation factor *p* for detectors has only been vigorously studied for electron beams and for photon beams under the condition of transient charged particle equilibrium. These studies are mostly done for ionization chambers. More importantly, these conditions restrict the electron fluence distribution to be uniform across the detector. The detector convolution kernel expanded this to regions where electron fluence distribution is not uniform. However, substantial works remains to understand the beam quality dependence of the detector convolution kernel and more theoretical work such as Monte-Carlo simulation is needed to understand its origin.

VIII Acknowledgment

The author wishes to thank Alan Nahum and Bengt E Bjärngard for valuable advice on perturbation effects in dosimetry.

IX Bibliography

1. Alm Carlsson G, "Theoretical Basis for Dosimetry" in *The dosimetry of ionizing radiation*, vol. I ed. Kase KR, Bjärngard BE, and Attix FH (Orlando FL: Academic Press 1985) pp1 –75.
2. ICRU *Radiation Dosimetry: Electron beams with energies between 1 and 50 MeV*, ICRU Report 35 (Bethesda MD: International Commission on Radiation Units and Measurements, 1984).
3. Dutreix A and Bridier A "Dosimetry for external beams of Photon and Electron Radiation", vol. I ed. Kase KR, Bjärngard BE, and Attix FH (Orlando FL: Academic Press 1985) pp. 164-228.
4. Johns HE and Cunningham JR, *The Physics of Radiology*, (Springfield IL: Charles C Thomas Publisher 1983) 4th edition.
5. Nahum AE, "Perturbation Effects in dosimetry: Part I. Kilovoltage x-rays and electrons," Phys. Med. Biol. 41, 1531-1580, 1996.
6. Svensson H and Brahme A, "Recent Advances in Electron and Photon Dosimetry" in *Radiation Dosimetry: Physical and Biological Aspects,* ed. Orton C G (New York: Plenum 1986) pp87-170.
7. AAPM 1983 "A protocol for the determination of absorbed dose from high-energy photon and electron beams," Med. Phys. 10 741-771 (1983).
8. Bjärngard BE and Kase KR "Replacement correction factors for photon and electron dose measurement," Med. Phys. 12, 785-7, 1985.
9. Fano U, "Note on the Bragg-Gary Cavity Principle for Measuring Energy Dissipation," Radiat. Res. 1, 237-40, 1954.
10. Cunningham JR and Sontag MR "Displacement corrections used in absorbed dose determination," Med. Phys. 7, 672-6, 1980.
11. Johansson KA, Mattsson LO, Lindborg L and Svensson H, "Absorbed dose determination with ionization chambers in electron and photon beams having energies between 1 and 50 MeV in *National and International Standardization of Radiation Dosimetry* Vol. II (Vienna: IAEA 1978) pp243-269.
12. Skaggs LS "Depth dose of electrons from the betatron," Radiology 53, 868-73, 1949.
13. Hettinger G, Petterson C and Svensson H, "Displacement effect of thimble chambers exposed to a photon or electron beam from a betatron," Acta Radiol. Ther. Phys. Biol. 6, 61-4, 1967.
14. IAEA 1987 "Absorbed Dose Determination in Photon and Electron Beams: An International Code of Practice", Technical Reports Series No. 277 (Vienna: International Atomic Energy Agency).
15. Andreo P "The status of high-energy photon and electron beam dosimetry five years after the publication of the IAEA code of practice", IAEA TECDOC *Review of data and methods recommended in the International Code of Practice* (Vienna: International Atomic Energy Agency, 1993).
16. Dutreix A "Problems of high-energy x-ray beam dosimetry" in *High-Energy Photons and Electrons* ed. Kramer S, Suntharalingam N, and Zinninger GF (New York: John Wiley 1976) pp. 203-14
17. McEwan AC "A theoretical study of cavity chamber correction factors for photon beam absorbed dose determination," Phys. Med. Biol. 25 39-50, 1980.
18. Zotelief J, Engel AC and Broerse JJ "Effective measuring point of ion chambers for photon dosimetry in phantoms," Br. J. Radiol. 53, 580-583, 1980.
19. Zoetelief J, Eagels AC, and Broerse JJ "Displacement corrections for spherical ionization chambers in phantoms irradiated with neutron and photon beams" in *Biomedical Dosimetry: Physical Aspects, Instrumentation, Calibration* SM249/38 (Vienna: International Atomic Energy Agency, 1981) pp. 125-38.
20. Sibata CH, Mota HC, Beddar AS, Higgins PD, and Shin KH, "Influence of detector size in photon beam profile measurements," Phys. Med. Biol. 36, 621-31, 1991.
21. Higgins PD, Sibata CH, Siskind L, Sohn JW, "Deconvolution of detector size effect for small field measurement," Med. Phys. 22, 1663-66, 1995.
22. Chang K-S, Yin F-F, Nie K-W, "The effect of detector size to the broadening of the penumbra – a computer simulated study," Med. Phys. 23, 1407-11, 1996.

23. Charland P, El-Khatib E, and Wolters J "The use of deconvolution and total least squares in recovering a radiation detector line spread function," Med. Phys. 25, 152-60, 1998.
24. Garcia-Vicente F, Delgado JM and Peraza C, "Experimental determination of the convolution kernel for the study of the spatial response of a detector," Med. Phys. 25, 202-207, 1998.
25. Dawson DJ, Harper JM, and Akinradewo AC, "Analysis of physical parameters associated with the measurement of high-energy x-ray penumbra," Med. Phys. 11, 491 – 497, 1984.
26. Rikner G "Silicon diodes as detectors in relative dosimetry of photon, electron and proton radiation fields" Ph.D. thesis Uppsala University, 1983.
27. Velkley DE, Manson DJ, Purdy JA, and Oliver, Jr GD, "Build-up region of megavoltage photon radiation sources," Med. Phys. 2, 14-19, 1975.
28. Nilsson B and Montelius A, "Fluence perturbation in photon beams under nonequilibrium conditions," Med. Phys. 13, 191-195, (1985).
29. Rogers DWO "Calibration of parallel-plate chambers: Resolution of several problems by using Monte Carlo calculations," Med. Phys. 19, 889-899, 1992.
30. Mellenberg Jr. DE "Determination of build-up region over-response corrections for a Markus-type chamber," Med. Phys. 17, 1041-1044, 1990.
31. Gerbi BJ, "The response characteristics of a newly designed plane-parallel ionization chamber in high-energy photon and electron beams," Med. Phys. 20, 1411-1415, 1993.
32. Gerbi BJ and Kahn FM, "Measurement of dose in the buildup region using fixed-separation plane-parallel ionization chambers," Med. Phys. 17, 17-26, 1990.
33. Rawlinson JA, Arlen D, and Newcombe D, "Design of parallel plate ion chambers for buildup measurements in megavoltage photon beams," Med. Phys. 19, 641-648, 1992.
34. Gerbi BJ and Kahn FM "Plane-parallel ionization chamber response in the buildup region of obliquely incident photon beams," Med. Phys. 24, 873-878, 1997.
35. Wickman G and Holmstrom T, "Polarity effect in plane-parallel ionization chambers using or a dielectric liquid as ionization medium," Med. Phys. 19, 637-640, 1992.
36. Aget H and Rosenwald, "Polarity effect for various ionization chambers with multiple irradiation conditions in electron beams," Med. Phys. 18, 67-72, 1991.
37. Galbraith DM, Rawlinson JA, and Munro P, "Dose errors to charge storage in electron irradiated plastic phantoms," Med. Phys. 11, 197-203, 1984.
38. Mattsson LO and Svensson, "Charge build-up effects in insulating phantom materials," Acta Radiol. Oncol. 23, 393-399, 1984.
39. Gerbi BJ and Kahn FM, "The polarity effect for commercially available plane-parallel ionization chambers," Med. Phys. 14, 210-215, 1987.
40. Almond PR, Attix FH, Humphries LJ, Kubo H, Nath R, Goetsch S, Rogers DWO, "The calibration and use of plane-parallel ionization chambers for dosimetry of electron beams: An extension of the 1983 AAPM protocol report of AAPM Radiation Therapy Committee Task Group No. 39," Med. Phys. 21, 1251-1260, 1994.
41. Mattsson LO, Johansson K-A, and Svensson H, "Calibration and use of plane-parallel ionization chambers for the determination of absorbed dose in electron beams," Acta Radiol. Oncol. 20, 385-99, 1981.
42. ICRU *Stopping powers for Electrons and Positrons*, ICRU Report 37 (Bethesda MD: International Commission on Radiation Units and Measurements, 1984).
43. Metcalfe P, Kron T, Elliott A, and Wong T, "Dosimetry of 6-MV x-ray beam penumbra," Med. Phys. 20, 1439-1442, 1993.
44. Kron T, Elliott A, and Metcalf P, "The penumbra of a 6-MV x-ray beam as measured by thermoluminescent dosimetry and evaluated using an inverse square root function," Med. Phys. 20, 1429-1438, 1993.
45. Zhu TC, Liu C, Bova F, Palta J, "Convolution based correction to ionization chamber measured output for small fields," Med. Phys. 23, 1166, 1996.
46. Treuer H, Boessecke R, Schlegel W, Hartmann GH, Muller RP, and Sturm V, "The source-density function: determination from measured lateral dose distributions and use for convolution dosimetry," Phys. Med. Biol. 37, 1895-1909, 1992.
47. Bjärngard BE, Tsai JS, and Rice RK, "Doses on the central axis of narrow 6-MV x-ray beams," Med. Phys. 17, 794-799 1990.
48. Engler MJ and Jones GL, "Small-beam calibration by 0.6- and 0.2-cm^3 ionization chambers," Med. Phys. 11, 822-26, 1984.
49. Serago CF, Houdek PV, Hartmann GH, Saini DS, Serago ME, and Kaydee A, "Tissue maximum ratios (and other parameters) of small circular 4, 6, 10, 15, and 24 MV x-ray beams for radiosurgery," Phys. Med. Biol. 37, 1943-1956, 1992.
50. Leavitt DD and Larsson L, "Evaluation of a diode detector array for measurement of dynamic wedge dose distributions," Med. Phys. 20, 381-382, 1993.
51. Liu H H, Lief EP, McCullough EC, "Measuring dose distributions for enhanced dynamic wedges using a multichamber detector array," Med. Phys. 24, 1515-1519, 1997.
52. Zhu TC, Ding L, Liu CR, Palta JR, Simon WE, Shi J: "Performance evaluation of a diode detector array for enhanced dynamic wedge dosimetry," Med. Phys. 24:1173-1180, 1997.
53. Watts RJ, "Evaluation of a diode detector array for use as a linear accelerator QC device," Med. Phys. 25, 247-250, 1998.
54. Profiler Model 1170 Operating instructions, Sun Nuclear Corp. Melbourne, FL. Oct 1996.